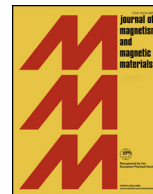




ELSEVIER

Contents lists available at ScienceDirect

Journal of Magnetism and Magnetic Materials

journal homepage: www.elsevier.com/locate/jmmm

Research articles

Size modulated Griffiths phase and spin dynamics in double perovskite $\text{Sm}_{1.5}\text{Ca}_{0.5}\text{CoMnO}_6$ R.C. Sahoo^a, Sananda Das^a, S.K. Giri^b, D. Paladhi^a, T.K. Nath^{a,*}^a Department of Physics, Indian Institute of Technology Kharagpur, West Bengal 721302, India^b Department of Materials Science and Metallurgy, University of Cambridge, 27 Charles Babbage Road, Cambridge CB3 0FS, United Kingdom

ARTICLE INFO

Keywords:

Magnetic oxides
Dynamic properties
Griffiths phase
Magnetic couplings

ABSTRACT

Griffiths phase like behavior has been investigated in details in size modulated $\text{Sm}_{1.5}\text{Ca}_{0.5}\text{CoMnO}_6$ double perovskite, having ferromagnetic entities in the paramagnetic matrix. Temperature dependent real and imaginary part of ac susceptibility confirms that $\text{Sm}_{1.5}\text{Ca}_{0.5}\text{CoMnO}_6$ -1150 °C bulk-sample has spin-glass like ordering below $T_g \sim 34.88(3)$ K. This glassy behavior is attributed to the antisite disorders ($\sim 7.12\%$) along with and magnetic frustration in the system. However, the ground state of $\text{Sm}_{1.5}\text{Ca}_{0.5}\text{CoMnO}_6$ -600 °C nanometric-sample is observed to be antiferromagnetic in nature due to the presence of large antisite disorder ($\sim 53.58\%$). The observed unusual co-existence of antiferromagnetism with Griffiths-like phase in $\text{Sm}_{1.5}\text{Ca}_{0.5}\text{CoMnO}_6$ -600 °C sample is rare in nature. Interesting magnetic spin dynamics and aging effect are also observed in both the compounds suggesting different spin relaxation processes in low temperature regime. The observed magnetism in these compounds can be tuned by nearest neighbor Co-O-Mn and/or Co-O-Co/Mn-O-Mn exchange interactions as well as the next nearest neighbor Co-O-O-Co/Mn-O-O-Mn interactions.

1. Introduction

In recent time one of the fascinating topics in the field of condensed matter physics is to explore various exciting features of complex magnetic oxides like Griffiths phase (GP), slow spin relaxation, aging and memory effects etc. [1–3]. Among them, the GP is one of the distinct magnetic state in which magnetization falls due to the completely random and competing magnetic interactions in the temperature range $T_C^{\text{Rand}} < T < T_G$, where T_C^{Rand} is the critical temperature for random ferromagnetic (FM) entities and T_G represents a temperature for the onset of completely random paramagnetic (PM) states [4,5]. In this intermediate temperature regime, the GP is microscopically distinguished by a FM cluster like system. This was first predicted theoretically in randomly diluted Ising ferromagnets by R. B. Griffiths in 1969 [6]. The presence of GP in magnetic materials is generally related to the competing magnetic interactions leading to FM entities. Moreover, the origin of GP varies from one material to other based on the synthesis conditions (size, dimension, shape, morphology, etc.), multiple crystallographic structure, quenched disorder and multi-magnetic phases. For example, de Teresa *et al.* have reported GP-like behavior in $(\text{La-Y/Tb})_{2/3}\text{Ca}_{1/3}\text{MnO}_3$ perovskite samples and they suggested competition between charge ordered antiferromagnet (AFM) and metallic FM appearing as nanoscale inhomogeneities in the PM regime [7]. The

$\text{Tb}_5\text{Si}_2\text{Ge}_2$ compound showed the GP-like state ($115 \text{ K} < T < 200 \text{ K}$) in actual PM region and it was originated from the crystallographic structural disorder along with competing intralayer and interlayer magnetic exchange interactions [8]. Ouyang *et al.* have reported that short range FM correlations and dynamic FM clusters are responsible for GP-like phase ($128 \text{ K} < T < 240 \text{ K}$) in binary compound Gd_5Ge_4 [9]. The $\text{Ca}_3\text{CoMnO}_6$ spin chain system showed GP-like feature ($13 \text{ K} < T < 125 \text{ K}$) due to short-range FM correlations [10]. A similar GP-like ordering ($6 \text{ K} < T < 12 \text{ K}$) was noticed in another spin-chain compound $\text{Sr}_3\text{CuRhO}_6$ [11]. On the other hand, the GP singularities have been observed in a non-Fermi-liquid system due to the interplay between the Kondo-like and RKKY interactions where both the magnetic anisotropy and disorder are present [12]. Recently, GP singularity has been identified in a dilute magnetic semiconductor $\text{Fe}_{1-x}\text{Co}_x\text{S}_2$ formation of which has been assigned to the clusters of localized ephemeral magnetic ordering [13].

The crystallographic disorder (including antisite defects (ASD)) in double perovskite compounds of general formula $\text{A}'_{2-x}\text{A}''_x\text{CoMnO}_6$ [A' = rare earth elements (Sm, La, Y, etc.) with oxidation state + 3 and A'' = alkaline-earth elements (Ca, Sr, Ba, etc.) with oxidation state + 2] can be introduced with the substitution of A'^{3+} by A''^{2+} with different ionic radii. This disorder induces distinct fascinating and complex properties like multi-glass behavior [14], phase separated

* Corresponding author.

E-mail address: tnath@phy.iitkgp.ernet.in (T.K. Nath).<https://doi.org/10.1016/j.jmmm.2018.08.060>

Received 18 June 2018; Received in revised form 10 August 2018; Accepted 22 August 2018

Available online 23 August 2018

0304-8853/ © 2018 Elsevier B.V. All rights reserved.

ferroelectricity [15], GP-like ordering [11], superconductivity [16], colossal magnetoresistance [17] and magnetic relaxation dynamics [14]. However, the magnetic properties of these materials are also influenced by the strong spin orbit coupling on the 3d transition metal ions and electron delocalization in the intrachain (Co-O-Mn) network. This also induces ASD in the double perovskite systems, *i.e.*, mislocation of either CoO₆ or MnO₆ octahedron inherently and forms interchain (Co-O-Co or Mn-O-Mn) interaction instead of intrachain interaction along each axis. The ASD is a common feature in most of the double perovskite systems and it destroys structural periodicity but introduces AFM superexchange coupling or/and magnetic frustration in the FM compound [18,19]. It leads to magnetic domain formation in the PM regime and as a result formation of GP and suppression of magnetization take place.

In this study, we report the size modulated structural, magnetic and spin dynamics of 25% Ca substituted Sm₂CoMnO₆ (Sm_{1.5}Ca_{0.5}CoMnO₆) double perovskite system. Interestingly, both the systems, Sm_{1.5}Ca_{0.5}CoMnO₆-1150 °C (say, SCCMO_B with a bulk average grain size of 1.5 μm) and Sm_{1.5}Ca_{0.5}CoMnO₆-600 °C (say, SCCMO_N with a nanometric average grain size of 20 nm) show GP-like ordering in a temperature regime $T_C^{\text{Rand}} < T < T_C$. Moreover, only SCCMO_B system exhibits glassy feature in the low temperature and we have tried to find out the possible origin of it. We have also investigated the magnetic aging behavior in the light of simple power law and stretched exponential models for both the samples [20].

2. Experimental details

Polycrystalline double perovskite Sm_{1.5}Ca_{0.5}CoMnO₆ (SCCMO) powders have been synthesized by chemical sol-gel route from the stoichiometric mixture of high purity Sm₂O₃, CaCO₃, Co(NO₃)₂·6H₂O, Mn(CH₃COO)₂·4H₂O precursor materials. The stoichiometric amount of Sm₂O₃ is dissolved into the minimum amount of nitric acid (HNO₃) to form Sm(NO₃)₃ and other precursors are dissolved in deionized water to get clear solutions. All the solutions are mixed together and then heated at 150 °C using a hot plate for 4 days. The obtained precursor black and fluffy powder is calcinated at 1150 °C for 10 h to get bulk powder of Sm_{1.5}Ca_{0.5}CoMnO₆ (SCCMO_B). The resin powder is calcinated at 600 °C for 6 h to get bulk powder of Sm_{1.5}Ca_{0.5}CoMnO₆ (SCCMO_N).

The crystallographic structural details of the sample have been investigated by rigorous high resolution x-ray diffraction (Panalytical x'pert pro HRXRD-I, PW 3040/60) using Cu-K_α radiation ($\lambda \sim 1.542 \text{ \AA}$) at 300 K, the field emission scanning electron microscopy (FESEM, SUPRA 40, Carl Zeiss SMT AG, Germany with a resolution of 1 nm) image and high resolution transmission electron microscopy (HRTEM, JEM2100 with a resolution of 1.9 Å). Electronic structure of the sample has been determined using X-ray photoelectron spectroscopy (XPS, PHI 5000 Versa Probe II Scanning). The magnetization measurements have been carried out by using SQUID magnetometry (Quantum Design, USA with resolution 10⁻⁸ emu) and Physical Property Measurement System (PPMS, Quantum Design, USA) in the temperature range of 5–325 K with a maximum field of ± 7 T. Before starting each magnetization measurement, the samples were heated above their respective Curie temperature to ensure the complete demagnetization state of the sample. The samples were also demagnetized by using oscillating field with an appropriate protocol.

3. Results and discussion

3.1. Structural properties

Room temperature HRXRD patterns of SCCMO_B and SCCMO_N samples display typical perovskite structure as shown in Fig. 1(a) and inset of Fig. 1(a), respectively. The XRD patterns show polycrystalline nature of the samples and broadening of the peaks with the decrease of calcinations temperature signifying the smaller average crystallite size.

Using Debye-Scherrer formula, the average crystallite size has been estimated to be ~21.4 nm for SCCMO_N sample. All the XRD spectra have been examined through Rietveld refinement using FullProf Suite programme. The observed reflections for both the samples are assigned to the small B-site disordered monoclinic crystal symmetry with space group P2₁/n (14). The presence of ASD in the B-site sublattice has been accounted to achieve the best fit. The obtained refined structural parameters for both the samples are listed in Table 1. All the peaks in XRD pattern of SCCMO_N sample are indexed well using this space group. From Table 1, we conclude that the Mn-O-Co angles in both the samples are found to be quite different in contrast to that found in the ordered Sm₂CoMnO₆ compound [21]. The interatomic distances (Co/Mn-O) for both the samples are not identical and more disorder in SCCMO_N, generally indicates the presence of oxygen vacancies or/and disorder in the crystal structure.

Fig. 1(b) shows the FESEM micrograph of SCCMO_N sample demonstrating almost uniform grains separated by grain boundaries. The calculated average grain size is ~20 nm (inset of Fig. 1(b)). In the Fig. 1(c), the ring pattern in the selective area electron diffraction (SAED) image confirms nanocrystalline nature of SCCMO_N samples. From this ring, we have calculated the average distance from two bright spots ~7.01 Å and corresponding lattice spacing $d \sim 0.28 \text{ nm}$. Fig. 1(d) shows the HRTEM lattice image of SCCMO_N, revealing the good crystallinity of the sample and the value of lattice spacing (~0.25 nm) corresponding to (1 1 2) plane is consistent with that estimated from SAED pattern. However, the estimated average grain size from FESEM micrograph of SCCMO_B is ~1.5 μm (not shown here) which is also consistent with our XRD result and previously reported results [22].

When an element of different ionic radius (Ca²⁺, radii ~ 1.0 Å) is substituted at Sm (Sm³⁺, radii ~ 1.08 Å) site in order to relieve the internal chemical stress, CoO₆ or MnO₆ octahedra cooperatively rotates (unequal Co-O and/or Mn-O bonds) and/or tilts (unequal Co/Mn-O-Co/Mn bond angles < 180°). Fig. 2(a) and (b) show the local environment of the SCCMO_B and SCCMO_N samples drawn using data from Table 1. The lattice parameters 'b' and 'c' are found to be smaller in SCCMO_N, while the parameter 'a' has increased as a result of enhancement of structural disorder. The inset of Fig. 2(a) shows crystal structure of SCCMO_B, where MnO₆ and CoO₆ octahedra are located at distinct preferential positions. The Co and Mn atoms are occupied along the three crystallographic directions at 2c (½, 0, 0) and 2d (0, ½, 0) positions, respectively. Here, the monoclinic structure consists of tilted and distorted CoO₆ and MnO₆ octahedra and are periodically arranged on the cubic edge. It makes the system consisting of reduced ASD. The inset of Fig. 2(b) shows crystal structure of SCCMO_N, where MnO₆ and CoO₆ octahedra are not located alternatively on the cubic edge and are assigned to large ASD (greater than 50%). The observed structural information of both the samples suggests that the system may contain a disordered phase along with ASD.

3.2. Comparative energy dispersive X-ray spectroscopy (EDX) study

EDX spectra analysis of SCCMO_B and SCCMO_N samples has been carried out to determine the chemical homogeneity of the polycrystalline samples as shown in the inset of Fig. 2(c) and (d), respectively. For both the samples, all the constituent elements are present without having any impurity element. Fig. 2(c) and (d) shows the normalized atomic and weight percentage plot of constituent elements for both the samples. The presence of percentage of elements matches quite well with the nominal stoichiometry of SCCMO samples. The calculated chemical formula of SCCMO_B is Sm_{1.5}Ca_{0.505}Co_{0.939}Mn_{1.09}O_{6.88} and that for SCCMO_N is Sm_{1.5}Ca_{0.496}Co_{0.898}Mn_{1.11}O_{6.8N}. The ratio of 3d transition metal elements (Co:Mn) in both systems is not perfectly 1:1. The estimated oxygen content, as calculated from charge balance, is ~5.404 for SCCMO_B and ~5.698 for SCCMO_N system. This confirms that the change in particle size or sintering temperature does affect the

Download English Version:

<https://daneshyari.com/en/article/8943583>

Download Persian Version:

<https://daneshyari.com/article/8943583>

[Daneshyari.com](https://daneshyari.com)